

Reinforcement Learning for Robot Navigation with Adaptive Execution Duration (AED) in a Semi-Markov Model

Yu'an Chen, Ruosong Ye, Ziyang Tao, Hongjian Liu, Guangda Chen, Jie Peng, Jun Ma,
Yu Zhang, Yanyong Zhang and Jianmin Ji*

Abstract—Deep reinforcement learning (DRL) algorithms have proven effective in robot navigation, especially in unknown environments, through directly mapping perception inputs into robot control commands. Most existing methods adopt uniform execution duration with robots taking commands at fixed intervals. As such, the length of execution duration becomes a crucial parameter to the navigation algorithm. In particular, if the duration is too short, then the navigation policy would be executed at a high frequency, with increased training difficulty and high computational cost. Meanwhile, if the duration is too long, then the policy becomes unable to handle complex situations, like those with crowded obstacles. It is thus tricky to find the “sweet” duration range; some duration values may render a DRL model to fail to find a navigation path. In this paper, we propose to employ adaptive execution duration to overcome this problem. Specifically, we formulate the navigation task as a Semi-Markov Decision Process (SMDP) problem to handle adaptive execution duration. We also improve the distributed proximal policy optimization (DPPO) algorithm and provide its theoretical guarantee for the specified SMDP problem. We evaluate our approach both in the simulator and on an actual robot. The results show that our approach outperforms the other DRL-based method (with fixed execution duration) by 10.3% in terms of the navigation success rate.

I. INTRODUCTION

Autonomous robot navigation with a complete map has been well studied [1] in the last few years. However, maps that have the global knowledge are not always available in many situations, such as in search and rescue scenarios or rapidly changing environments. Conventional path planning approaches mostly rely on accurate, static models of the environments, and they often fail to function when such models (i.e., maps) are not known [1]. As a result, robust navigation approaches in unknown environments are needed to help navigate the robot to its target using local perception capabilities from sensors such as 2D laser or cameras.

In recent years, deep reinforcement learning (DRL) algorithms have been successfully applied to navigation in unknown environments [2], [3], [4]. These data-driven methods learn their navigation policy by trial-and-error explorations combined with carefully designed reward signals. The policy usually directly maps the perception inputs, like 2D laser data or local costmap [5] to low-level control commands, such as the translational and rotational velocities that the robot aims to achieve. However, these methods usually execute their control commands at fixed intervals and formulate the problem as a Markov Decision Process (MDP), which could

School of Computer Science and Technology, University of Science and Technology of China, Hefei, 230026, China

* Corresponding authors. {jianmin}@ustc.edu.cn

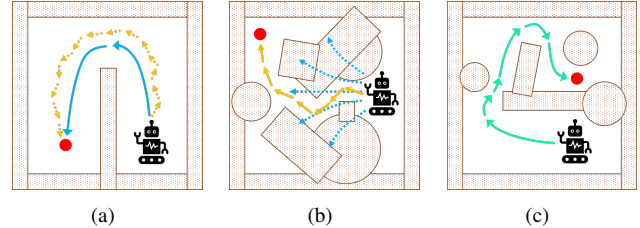


Fig. 1. In this work, we propose a navigation method that can adjust the execution duration (or control frequency) to better adapt to unknown environments. The above sketches give an example to explain why we need adaptive duration, where red dots denote the targets, yellow arrows denote short-duration steps, blue arrows denote long-duration steps and green arrows denote adaptive duration steps. (a) An environment is suitable for the robot to take long-duration steps. (b) An environment is suitable for the robot to take short-duration steps. (c) An environment requires the robot to adaptive change its execution duration.

potentially limit their performance when the environment has non-uniform properties. For example, as shown in Fig. 1(a), the robot is supposed to first depart from the target before it can finally reach the target, for which it is hard for greedy policies to find a solution. Instead, the robot needs to explore to reach its target. In such a spacious and empty environment, the robot is expected to reach the target much faster when exploring with longer duration steps. On the contrary, when the environment is filled with obstacles, the robot is more efficient with shorter duration steps. Fig. 1(b) illustrates such a crowded environment and a robot that cannot find its way with long-duration steps.

Obviously, different environments call for different execution step sizes. More importantly, for an environment that is complex enough to have multiple spatial features and obstacle densities, we may not be able to find a single step size that is minima for the entire environment. Instead, as shown in Fig. 1(c), if the robot adjusts its step size as its surrounding changes, it could potentially navigate the robot in more challenging environments and reach the target more efficiently with less planning time (sum of computing time of each step) and wall time (actual time from the start to the arrival).

In this paper, we propose Adaptive Execution Duration (AED), a DRL-based navigation method that can rapidly adapt to unknown surrounding environments by dynamically adjusting the execution duration. Specifically, the trained model learns to adjust the duration according to how the obstacles are distributed in the robot’s current sensing region, i.e., adopting a shorter duration for regions with dense

obstacles while a longer duration for sparse regions. Once the next execution duration is determined, robots can move at the maximum allowed speed (either translational speed or rotational speed). Hence, compared to policies with a fixed duration, AED can better deal with complex environments, striking a nice balance between how well a robot can avoid obstacles and how fast it can reach the destination.

To suitably adapt the execution duration, we propose to formulate the navigation task as a Semi-Markov Decision Process (SMDP) problem [6], each of whose actions consists of three components: translational velocity, rotational velocity, and duration. Please note that, during each duration, the robot also needs to further refine its movement to avoid unexpected collisions. As such, the robot may end an action before completing the given duration, which preserves the semi-Markov property of the decision process: the dynamics of the world is specified by the transition probability function $P(s', \tau' | s, a)$ for the time τ' when the robot ends an action.

This is not the first time that the navigation problem is formulated as a SMDP problem; in fact, in previous works such as those in [7], [8], [9], SMDP models were used. However, most of the previous models adopt a set of *predefined discrete* actions. Such a discrete action space can simplify the problem and speed up the planning process but limits the potential of these algorithms to adapt to more complex and diverse environments. On the contrary, our approach allows the robot to choose proper execution duration for *continuous* actions to dynamically adapt to its surroundings. That is, our actions are more flexible and not limited by a predefined action set.

In order to efficiently adapt the execution duration, we face the following two main challenges: the large volume of samples that are required, as well as the difficulty of obtaining stable improvement despite the nonstationarity of the samples. We address the first challenge by devising a transformation that converts our 3D actions to 2D virtual actions in the trajectory parameter space (TP-space) [10]. Such a conversion can effectively compress the action space and reduce the number of required samples (Fig. 2). We address the second challenge by improving the distributed proximal policy optimization (DPPO) algorithm [11] in the SMDP problem. The key to obtaining stable improvement is to have a good estimation of the policy gradient. The default policy estimator of DPPO is Generalized advantage estimation (GAE) [12], which can substantially reduce the variance of policy gradient estimates at the cost of acceptable bias. However, the original GAE focuses on MDP problems, and we revise the discount rate in the policy gradient estimates to suit our problem. We also provide the theoretical guarantee of the modified GAE in SMDPs.

We evaluate our approach under multiple scenarios both in the simulator and on a differential-drive mobile robot in the real world. We compare AED with a classical motion planner, the dynamic window approach (DWA) [13], as well as a DRL-based approach with fixed execution duration [14]. The experimental results show that the ability to adjust execution duration in AED can greatly improve

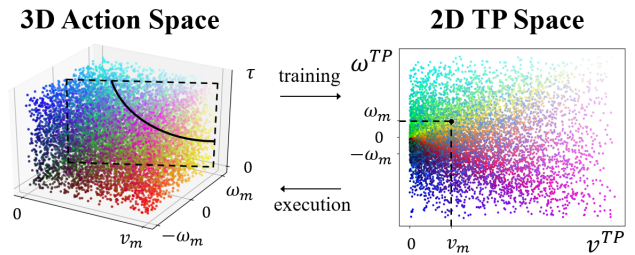


Fig. 2. We formulate the navigation task as a SMDP problem, whose action space is three dimensional, i.e., translational velocity $v \in [0, v_m]$, rotational velocity $\omega \in [-\omega_m, \omega_m]$, and duration $\tau \in (0, +\infty)$. One challenge of solving this SMDP problem with DRL is the numerous samples typically required result from the high dimensional action space. So we compress the 3D executable action to a 2D virtual action in TP space for planning and convert it back for actual execution. In the above pictures, each point of the 3D action space has a different color and is mapped to the point with the same color in 2D TP space. For example, a curve in the 3D action space can be converted to a point in the 2D TP space, which shows how we compress the action space. The details of the transformation are presented in Section III-C

the navigation performance mainly in the metric of success rate in unknown environments. We also conduct ablation experiments to demonstrate the effectiveness of (1) the transformation that converts 3D executable actions to 2D virtual actions in TP-space and (2) the modified GAE. In particular, the success rate is 10.3% higher in all the environments we have tested in. The demonstration video can be found at <https://youtu.be/toip5bFfJ1w>. Our main contributions are summarized as follows:

- We propose a DRL-based navigation method that can automatically adjust the execution duration of the robot. The experimental results show that the approach is efficient and outperforms the DRL-based method with fixed time duration in multiple environments.
- We formulate the navigation problem as a SMDP problem that allows the robot to select its proper execution duration. We also provide a transformation that converts a 3D executable action to a 2D virtual action in TP-space to reduce the training difficulty.
- We improve the DPPO algorithm for the specified SMDP problem by modifying its GAE to better estimate the policy gradient in SMDP.

II. RELATED WORK

A. DRL-based Navigation

DRL-based methods for navigation have been proposed with promising results [15]. In most existing DRL-based methods, a navigation policy is specified by a trained model that maps the perception inputs into the robot's low-level control commands. [2], [3], [4] use DRL to tackle with mapless navigation. [16] presents a DRL-based collision avoidance algorithm, which models the complex interactions with nearby agents. [17], [14] introduce a multi-stage training framework to optimize a decentralized multi-robot collision-avoidance policy. Please notice that control commands are executed for a fixed time duration in all of the above methods.

B. Navigation as SMDP

The navigation problem has been specified as a SMDP problem. [7] describes a navigation architecture based on Partially Observable Semi-Markov Decision Processes (POS-MDP) to realize avoidance in corridors. [18], [19] utilize inverse reinforcement learning (IRL) to estimate an appropriate reward function to improve robots' navigation performance. [8], [9] address the mapless navigation problem in the method of SMDP with Unawareness and Transfer (SMDPU-T). As mentioned in Section I, these methods require a set of *predefined discrete* actions, which simplifies the problem but limits the adaptive capacity of the algorithms. On the contrary, our AED can choose proper execution duration for *continuous* actions, rendering a more flexible navigation policy.

III. PRELIMINARIES

A. Semi-Markov Decision Process

A Semi-Markov Decision Process (SMDP) [6] is a tuple (S, A, P, R, T, γ) , where S is the state space, A is the action space, T is the transition time space, and $\gamma \in (0, 1]$ is the discount factor. We assume the environment has transition dynamics $P(s', \tau' | s, a)$ which is unknown to the agent, where τ' represents the time between taking action a in observed state s and arriving in the next state s' and can take a new action. In general, we are given the reward function $r = R(s, a, s')$ for the reward after observing s' . The goal throughout is to learn a policy maximizing long-term expected rewards $\mathbb{E}[\sum_{i=0}^{L-1} \gamma^i r_i]$ with a horizon $T = t_L$, where $t_0 = 0$ and $t_i = \sum_{j=0}^{i-1} \tau_j$.

B. Formulation of Navigation in SMDP

In this paper, we specify the navigation task as a SMDP problem. Specifically, an action a is formulated as a triple (v, ω, τ) , where v and ω denote the required translational and rotational velocities for the robot, and τ denotes the execution duration for both velocities. A state s consists of the pose of the robot, i.e., (x, y, θ) for the robot's position (x, y) and the orientation θ , as well as the corresponding observation of the robot at the position. If there is no collision during the execution, then the robot would execute the velocities v and ω for the time interval τ , which results in the next state s' . However, the robot needs to adjust its movement to avoid potential collisions during the execution and possibly ends an action before completing its given execution duration, which results in the transition dynamics $P(s', \tau' | s, a)$, with $\tau' \in [0, \tau]$ denoting the actual execution time. A policy $\pi(a | s)$ specifies the probability of taking action a at state s . The reward function R encourages the navigation policy to avoid collisions and arrive at the target position as soon as possible.

C. Trajectory Parameter Space with Velocities

To decrease the number of samples typically required, we convert the 3D executable actions to 2D virtual actions in the trajectory parameter space for planning and convert it back for actual execution.

A trajectory parameter space (TP-space) [10] is a 2D space where each point corresponds to a drivable trajectory for a robot. The basic idea is that a sequence of robot's pose in 3D space (x, y, θ) can be charted employing 2D manifolds in the parameter space of a family of trajectories.

In this paper, we consider differential-drive robots, which only move along circular trajectories due to their movement restrictions. Then we can use a 2D virtual action (v^{TP}, ω^{TP}) to parameterize the trajectories with a predefined fixed time interval τ^{TP} . We call it virtual action because v^{TP} and ω^{TP} are virtual translational and rotational velocities in TP-space, which are not limited by the actual robot's maximum translational velocity v_m and rotational velocity ω_m .

In order to conduct the 3D-to-2D conversion, we first employ a fixed time interval in the 3D space, τ^{TP} , as the *virtual duration*. Starting from the initial point $(0, 0)$, we can convert a virtual action (v^{TP}, ω^{TP}) to an executable action (v, ω, τ) , i.e.,

$$v = \frac{v^{TP}}{k}, \quad \omega = \frac{\omega^{TP}}{k}, \quad \tau = k \tau^{TP}, \quad (1)$$

where k is a real number, with $k = \max(\frac{v^{TP}}{v_m}, \frac{\omega^{TP}}{\omega_m})$.

Note that, *virtual duration* τ^{TP} is a fixed time interval in TP-space. Meanwhile the execution duration τ computed by τ^{TP} and (v^{TP}, ω^{TP}) is flexible, as k is variable w.r.t. (v^{TP}, ω^{TP}) . Then we utilize a 2D virtual action (v^{TP}, ω^{TP}) in TP-space to specify a 3D executable action (v, ω, τ) for the robot w.r.t. a virtual duration τ^{TP} . This translation allows us to train a model that outputs 2D virtual actions and transform these outputs into the robot's executable actions in execution.

IV. EXTENDING PG AND GAE FOR SMDP

In reinforcement learning, events (e.g., a robot collides) in the far future are weighted less than events in the immediate future. In our scheme, an action's execution duration can determine when an event will take place in the future, and thus also determine the event's weight. However, original generalized advantage estimation (GAE) [12] focuses on MDPs and does not consider such impact of execution duration. To address this issue, we extend the policy gradient (PG) theory for SMDPs and improve GAE to better estimate the policy gradient in SMDPs. We provide the theoretical guarantee for the improved GAE and show that it does not introduce extra bias conditionally.

A. Extending Policy Gradient

Before improving GAE for SMDPs, we extend the policy gradient theory for SMDPs first. The main extension stems from considering the dynamic execution duration and the probability of terminating an action before completion.

As reviewed in Section III, the optimal policy in SMDP is to maximize the expected cumulative discounted reward (return), i.e., $\mathbb{E}[\sum_{i=0}^{L-1} \gamma^i r_i]$ for a horizon $T = t_L$, where $t_0 = 0$ and $t_i = \sum_{j=0}^{i-1} \tau_j$. Given a parametric policy π_θ , its expected return is determined by the distribution of possible episodes ρ w.r.t. its parameters θ . In particular, we can formulate the objective function following Monte Carlo method [20]:

$$\bar{R}_\theta = \mathbb{E} \left[\sum_{i=0}^{L-1} \gamma^i r_i \right] = \mathbb{E}_{\rho \sim p_\theta(\rho)} [R(\rho)] = \sum_{\rho} R(\rho) p_\theta(\rho),$$

where the episode ρ specifies a sequence of states and actions, i.e., $\langle s_{t_0}, a_{t_0}, s_{t_1}, \dots, a_{t_{L-1}}, s_{t_L} \rangle$, $p_\theta(\rho)$ denotes the probability of producing an episode ρ w.r.t. π_θ , and $R(\rho)$ denotes the cumulative discounted reward of the episode ρ . Then the gradient of this objective function is ¹:

$$\nabla \bar{R}_\theta = \frac{1}{N} \sum_{n=1}^N \sum_{i=0}^{L_n-1} \Psi_i \nabla \log \pi_\theta(a_i^n | s_i^n), \quad (2)$$

where N denotes the number of sampled episodes, L_n denotes the number of actions in the n th episode, s_i^n and a_i^n denote the corresponding state and action in the n th episode, Ψ_i denotes a policy estimation function.

Note that, Ψ_i can be specified by multiple functions, including the return of the episode $\sum_{i=0}^{L-1} \gamma^i r_{t_i}$, the one-step TD residual $r_i + \gamma^{t_i} V^{\pi_\theta}(s_{t_i+\tau_i}) - V^{\pi_\theta}(s_{t_i})$, the state-action value function $Q^{\pi_\theta}(s_i, a_i)$, and the advantage function $A^{\pi_\theta}(s_i, a_i)$. In this paper, we specify Ψ_i as the advantage function $A^{\pi_\theta}(s_i, a_i)$ to estimate the policy gradient.

B. Improving Generalized Advantage Estimation

Generalized advantage estimation (GAE) introduced in [12] is a robust estimate of the advantage function in Markov Decision Processes (MDP). In this section, we introduce extended generalized advantage estimation (EGAE), a variation of GAE that is better suited to estimate the advantage function A^{π_θ} in SMDP.

First, we introduce the definitions of the state value function V^{π_θ} , the state-action value function Q^{π_θ} , and the advantage function A^{π_θ} in SMDP, i.e.,

$$\begin{aligned} V^{\pi_\theta}(s_i) &= \mathbb{E}_{\rho \sim p_\theta(\rho(s_i))} \left[\sum_{l=0}^{\infty} \gamma^l r_{t_{i+l}} \right], \\ Q^{\pi_\theta}(s_i, a_i) &= \mathbb{E}_{\rho \sim p_\theta(\rho(s_i, a_i))} \left[\sum_{l=0}^{\infty} \gamma^l r_{t_{i+l}} \right], \\ A^{\pi_\theta}(s_i, a_i) &= Q^{\pi_\theta}(s_i, a_i) - V^{\pi_\theta}(s_i), \end{aligned}$$

where $\rho(s_i)$ (resp. $\rho(s_i, a_i)$) denotes the episode starting from the state s_i (resp. the state s_i and the action a_i), and $z_l^{i+l} = t_{i+l} - t_i = \sum_{j=i}^{j=i+l-1} \tau_j$.

An advantage estimator \hat{A}_ρ denotes the estimation of the advantage function by considering the episode ρ . Following the notion γ -just in [12], we can define E-just for the advantage estimator \hat{A}_ρ in SMDP, so that it is an estimator that does not introduce bias when we use it in place of A^{π_θ} .

Definition 1: The estimator \hat{A}_ρ is E-just if

$$\begin{aligned} \mathbb{E}_{\rho \sim p_\theta(\rho(s_0, a_0))} [\hat{A}_\rho(s_i, a_i) \nabla \log \pi_\theta(a_i | s_i)] \\ = \mathbb{E}_{\rho \sim p_\theta(\rho(s_0, a_0))} [A^{\pi_\theta}(s_i, a_i) \nabla \log \pi_\theta(a_i | s_i)]. \end{aligned}$$

Now we introduce EGAE that improves GAE to better estimate the advantage function A^{π_θ} in SMDP.

Given an approximate state value function \hat{V} , for each $k \geq 1$ we define

$$\begin{aligned} \hat{A}_\rho^{(k)}(s_i, a_i) &= \sum_{l=0}^{k-1} \gamma^l \delta_{i+l}^{\hat{V}} \\ &= -\hat{V}(s_i) + r_i + \gamma^1 r_{t_{i+1}} + \dots + \gamma^{k-1} r_{t_{i+k-1}} + \gamma^k \hat{V}(s_{t_{i+k}}), \end{aligned}$$

¹The detailed derivation process of Equation (2) is specified in Appendix Material at <http://staff.ustc.edu.cn/~jianmin/supple/appendix.pdf>.

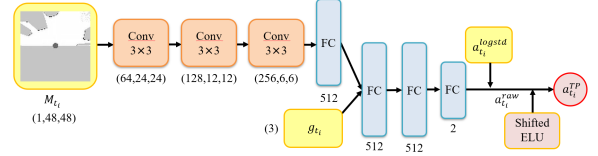


Fig. 3. We use DPPO to solve the navigation problem modeled in a SMDP. Above is the architecture of our policy network. The input of the network is s_i , which consists of the local grid map M_{t_i} and the relative target pose g_{t_i} . The output of the last layer is added by a Gaussian noisy a_i^{logstd} and get the raw action a_i^{raw} . Then we use a specified activation function with ELU to process it and get the virtual action a_i^{TP} .

where $\delta_{i+l}^{\hat{V}} = r_{t_{i+l}} + \gamma^{z_l^{i+l}} \hat{V}(s_{t_{i+l+1}}) - \hat{V}(s_{t_{i+l}})$. Note that, $z_l^{i+l} = (t_{i+l} - t_i) + (t_{i+l+1} - t_{i+l}) = t_{i+l+1} - t_i = z_{l+1}^i$. In particular,

$$\begin{aligned} \hat{A}_\rho^{(1)}(s_i, a_i) &= \delta_i^{\hat{V}}, \\ \hat{A}_\rho^{(\infty)}(s_i, a_i) &= -\hat{V}(s_i) + \sum_{l=0}^{\infty} \gamma^l r_{t_{i+l}}. \end{aligned}$$

Then we define EGAE $\hat{A}_\rho^{\text{EGAE}}$

$$\begin{aligned} \hat{A}_\rho^{\text{EGAE}}(s_i, a_i) &= (1 - \lambda) \left(\hat{A}_\rho^{(1)}(s_i, a_i) + \lambda \hat{A}_\rho^{(2)}(s_i, a_i) + \dots \right) \\ &= (1 - \lambda) \left(\delta_i^{\hat{V}} + \lambda \left(\delta_i^{\hat{V}} + \gamma^{z_1^i} \delta_{i+1}^{\hat{V}} \right) + \dots \right) \\ &= \sum_{l=0}^{\infty} \gamma^l \lambda^l \delta_{i+l}^{\hat{V}}, \end{aligned}$$

where $\lambda \in [0, 1]$ is a hyperparameter representing the compromise between bias and variance. Similar to the discussion in [12], the increase of λ results in the increase of the variance and the decrease of the bias.

Theorem 1: The estimator EGAE $\hat{A}_\rho^{\text{EGAE}}$ is E-just when $\lambda = 1$ or \hat{V} is accurate, i.e., $\hat{V} = V^{\pi_\theta}$.

Theorem 1² provides the theoretical guarantee for EGAE that it could be unbiased when we use it in place of A^{π_θ} .

V. DISTRIBUTED PROXIMAL POLICY OPTIMIZATION

In this section, we present details on how to apply Distributed Proximal Policy Optimization (DPPO) [11] to the SMDP problem with the two enhancement techniques – i.e., the transformation that converts a 3D executable action (v, ω, τ) to a 2D virtual action (v^{TP}, ω^{TP}) as well as the adoption of EGAE.

A. Reinforcement Learning Components

A state s_i consists of the egocentric local grid map M_{t_i} and the relative target pose g_{t_i} of the robot as shown in the Fig. 3. In our experiment, M_{t_i} is generated from the result of a 2D laser scan with a 180-degree horizontal Field of View (FOV).

An executable action a_i for the robot is a triple $(v_i, \omega_i, \tau_i^d)$. A virtual action a_i^{TP} is a pair $(v_i^{TP}, \omega_i^{TP})$, that is considered as the output of the network. Note that, a_i^{TP}

²The proof is specified in Appendix Material at <http://staff.ustc.edu.cn/~jianmin/supple/appendix.pdf> due to space limitations.

can be converted to a_{t_i} for execution by Equation (1). In the last layer of the network, we specify an activation function with exponential linear unit (ELU) [21] for the raw action $a_{t_i}^{raw}$, which is a pair $(v_{t_i}^{raw}, \omega_{t_i}^{raw})$ at the last layer of the network, i.e.,

$$\begin{aligned} v_{t_i}^{TP} &= \begin{cases} 0.2e^{5v_{t_i}^{raw}-1} & \text{if } v_{t_i}^{raw} < 0.2, \\ v_{t_i}^{raw} & \text{otherwise,} \end{cases} \\ \omega_{t_i}^{TP} &= \omega_{t_i}^{raw}. \end{aligned} \quad (3)$$

The reward r_{t_i} consists of four components, i.e.,

$$\begin{aligned} r_{t_i} &= r_{t_i}^{app} + r_{t_i}^{arr} + r_{t_i}^{col} + r_{t_i}^{step}, \\ r_{t_i}^{app} &= \varepsilon_a (\|p_{t_{i-1}} - p_g\| - \|p_{t_i} - p_g\|), \\ r_{t_i}^{arr} &= \begin{cases} r_{arr} & \text{if } \|p_{t_i} - p_g\| < 0.3, \\ 0 & \text{otherwise,} \end{cases} \\ r_{t_i}^{col} &= \begin{cases} r_{col} & \text{if collision,} \\ 0 & \text{otherwise,} \end{cases} \\ r_{t_i}^{step} &= -\varepsilon_t \tau_{t_i} - \varepsilon_\tau \tau^{TP}, \end{aligned}$$

where p_{t_i} (resp. $p_{g_{t_i}}$) denotes the position of the robot (resp. target g_{t_i}) at the current time t_i , $r_{arr} > 0$, $r_{col} < 0$, $\varepsilon_a > 0$, $\varepsilon_t > 0$, and $\varepsilon_\tau > 0$ are hyperparameters.

In particular, $r_{t_i}^{app}$ defines the penalty for departure from the target, $r_{t_i}^{arr}$ defines the reward for arrival at the target, r_{col} defines the penalty for collisions, and $r_{t_i}^{step}$ defines a minor penalty for each time step to encourage short paths. In our experiment, we set $r_{arr} = 500$, $r_{col} = -500$, $\varepsilon_a = 200$, $\varepsilon_t = 12$, and $\varepsilon_\tau = 10$.

B. Network Architecture

The architecture of our policy network π_θ is shown in Figure 3. Note that, the activation function of the last layer is specified in Equation (3). Meanwhile, our value network has the same architecture as the policy network, except that the last layer is modified to only output the value function V_ϕ without the Gaussian noise and the activation function.

C. Training Process

We replace GAE with EGAE in DPPO. Then the objective function for the policy network π_θ is

$$\begin{aligned} L_{\theta_k}^{CLIP}(\theta) &= \mathbb{E}_{s,a \sim \theta_k} \left[\min \left(\frac{\pi_\theta(a|s)}{\pi_{\theta_k}(a|s)} \hat{A}_p^{\text{EGAE}}(s,a), \right. \right. \\ &\quad \left. \left. g(\varepsilon, \hat{A}_p^{\text{EGAE}}(s,a)) \right) \right], \\ g(\varepsilon, \hat{A}) &= \begin{cases} (1+\varepsilon)\hat{A} & \text{if } \hat{A} \geq 0 \\ (1-\varepsilon)\hat{A} & \text{otherwise,} \end{cases} \end{aligned}$$

where θ_k denotes the parameters of the policy at the k th iteration and ε is the clip ratio.

As illustrated in Figure 4(a), we train the networks in environments that are constructed by a customized simulator based on OpenCV [22]. In particular, the simulator can load an environment as a gray image, where obstacles and robots are specified as corresponding pixels in the image. In DPPO, the algorithm collects experiences in a distributed setting from multiple environments where robots share the same navigation policy π_θ .

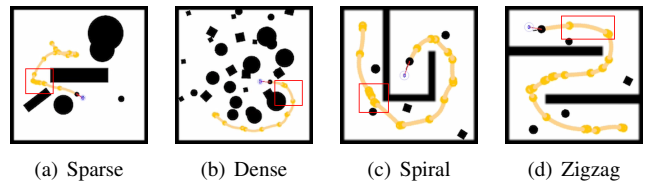


Fig. 4. We consider four scenarios in our experiments and their global top views are shown as the above, where yellow curves denote the navigation paths of the robot and the distance between two adjacent yellow dots denotes the corresponding execution duration. We can see in the red boxes that our robot can adjust its action execution duration to adapt to multiple spatial features and obstacle densities. More importantly, the trajectories in four scenarios are performed by an identical agent trained only in (a).

VI. SIMULATION EVALUATION

In this section, we present the simulation evaluation methods and results.

We train the AED with hyperparameters listed in Table I. Both the policy and value networks are implemented in TensorFlow [23] and trained with the Adam optimizer [24] on a computer with i7-9900 CPU and Nvidia Titan RTX GPU. It takes around 10 hours to run about 1200 iterations in DPPO, when the networks converge in training environments. We set $v_m = 0.6$ m/s and $\omega_m = 0.9$ rad/s for the robot in both simulations and real-world experiments. We did not add security policy (ending the action before collision) to the DRL-based methods in simulations.

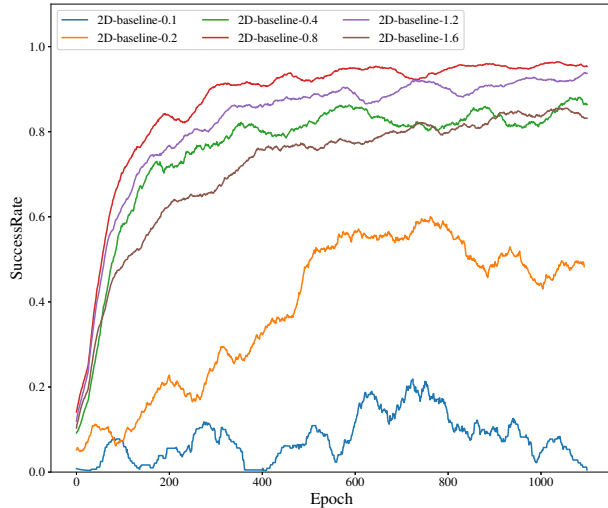
A. Training and Testing Scenarios

Figure 4 illustrates four different scenarios that are considered in our experiments. Please note that we only consider environments in the sparse scenario as training environments and evaluate the performance in these four scenarios:

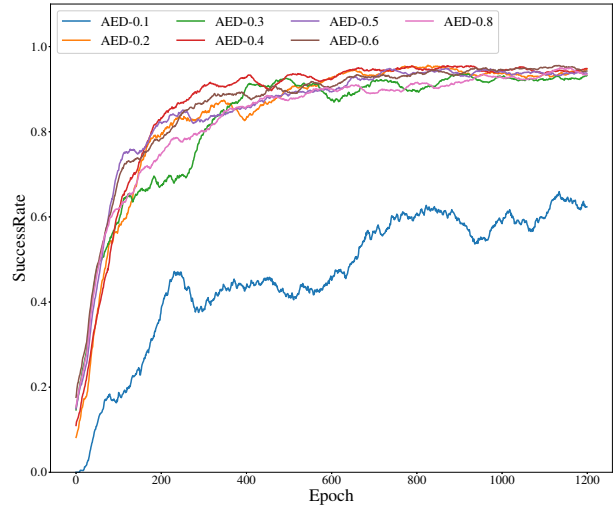
- **Sparse** scenarios contain environments that randomly choose locations for a small number of obstacles, the starting and target positions of the robot.
- **Dense** scenarios contain environments that randomly choose locations for a large number of obstacles, the starting and target positions of the robot.
- **Spiral** scenarios contain environments using a spiral map with randomly placed obstacles, where the starting and target positions of the robot are fixed in the map.

TABLE I
HYPERPARAMETERS

Hyperparameter	Value
Learning rate for π_θ	3×10^{-4}
Learning rate for V_ϕ	1×10^{-3}
γ in EGAE	0.975
λ in EGAE	0.95
Clip ratio ε	0.2
Batch size	2000
Image size	48×48
Episode length	200
Training iterations per epoch for π_θ	80
Training iterations per epoch for V_ϕ	80



(a) Learning curves of 2D Baseline with different values of Δt .



(b) Learning curves of AED with different values of τ^{TP} .

Fig. 5. The Learning curves of normal fixed execution duration method and our AED are shown in the above. We can see the learning results of the fixed execution duration method is sensitive to the value of the fixed duration Δt . Many values render poor policy with a low success rate. On the contrary, our adaptive duration method is robust to most values of its parameter τ^{TP} and converges to a similar high success rate.

- **Zigzag** scenarios contain environments using a zigzag map with randomly placed obstacles, where the starting and target positions of the robot are fixed in the map.

B. Comparison Baselines and Evaluation Metrics

We compare AED with three baseline methods, i.e.,

- **DWA Baseline** (Δt): an elegant and classical local planner, DWA, with a fixed execution duration Δt . The input of DWA is the same as the following three methods.
- **2D Baseline** (Δt): the DPPO-based navigation method with a fixed execution duration Δt proposed in [14]. Note that, the original GAE is applied in it.
- **3D Baseline** ($\Delta t \times n$): a straightforward extension of 2D Baseline (Δt) by adding a new dimension n to the output layer, where the desired execution duration is $\Delta t \times n$. EGAE is also applied in this extension.
- **AED** (τ^{TP}): AED with different values of the virtual duration τ^{TP} . Note that, the decrease of the virtual duration increases the sampling probability of short execution duration, which would affect the performance. However, we will show that it is much easier to choose a proper τ^{TP} than Δt for the 2D Baseline in experiments.

All DRL-based methods share the same reward function defined in Section V-A for a fair comparison. We train these models in the same set of environments in the Sparse scenario and test their performance in the same set of environments for all four scenarios.

We use success rate (SR) to evaluate the performance, which is the ratio of tests that the robot reaches its target without any collision.

C. Training Results

Fig. 5 shows the learning curves of the 2D baseline (with different execution duration Δt values) and AED (with

different virtual duration τ^{TP} values) in sparse environments.

We observe in Fig. 5(a) that even though the 2D baseline can converge to a higher SR value than the AED variations, the performance of the 2D baseline is highly sensitive to the choice of execution duration Δt . There exists a “sweet duration” range for the execution duration choice, e.g., around $\Delta t = 0.8$ in Fig. 5(a). If the actual duration is smaller than this range, it will have too many steps and unnecessarily complicate the navigation task; when the duration is larger, it becomes more likely to overshoot and miss the turning points. As a consequence, it would take more effort to find the sweet duration value in reality, especially when the robot faces complex environments.

On the contrary, Figure 5(b) shows that most virtual duration values τ^{TP} result in similar learning curves and converge to similar SR values. As a result, we do not have to put too much effort into choosing the virtual duration value; a large range of values will work reasonably well.

D. Test Results

Table II summarizes the test results using all four different scenarios, in which we performed 500 tests for each model under every scenario. We detail our observations below:

1) **The performance of AED:** Due to the benefit of having adaptive execution duration, AED performs the best in most of the cases (except for the sparse environments). In particular, the best average SR value is 94.0%, much higher than the best average SR value for 2D models (83.7%). More importantly, we find that many virtual duration values lead to competitive SR results for AED, which again confirms the observation that we don’t need to put too much effort to find the best virtual duration value to achieve a good SR value.

2) **The performance of 2D baseline:** We observe the same trend here as in the training results. In all four sce-

narios, the SR value is sensitive to the choice of Δt . Across scenarios, the sweet duration value also varies. For example, 2D baseline (0.8) achieves the highest SR in the spiral and zigzag scenarios, and 2D baseline (0.4) is the best in the dense scenario, as a relatively smaller fixed duration is more suitable for avoiding crowded obstacles.

3) **The performance of 3D baseline:** When the 3D baseline models have the same δt values as the 2D baseline models, we observe that the former performs slightly better thanks to having adaptive execution duration. However, by converting 3D executable actions to 2D virtual actions and requiring fewer samples, our method significantly outperforms the 3D Baseline models.

4) **The performance of DWA:** DWA has inherent safety rules in that the robot is only allowed to take collision-free actions (assuming obstacles are static). However, DWA cannot achieve 100% SR as the robot may get trapped in the local optimum. Its guidance of heading towards the target may prevent the robot from navigating its way around big obstacles. This problem causes the SR value to drop to zero in spiral and zigzag scenarios.

E. Ablation Studies

We also conduct ablation studies to investigate the utility of several modifications we propose in our scheme. Specifically, ‘AED’ denotes AED (0.4) which has the highest SR value in testing scenarios. ‘ReLu’ means replacing the activation function with shifted ELU instead of ReLu [25], ‘TD(0)’ means replacing EGAE with TD(0), and ‘GAE’ means replacing EGAE with GAE. The results are shown in Table III. In general, we find the above modifications all lead to performance improvements.

ReLu clips the negative output values by the network to zero, which may lose some useful information that can be

utilized by ELU. Therefore, the SR of ‘ReLu’ in all scenarios is lower than ‘AED’. TD(0) estimates the advantage function with a low variance but high bias. Thus the SR of ‘TD(0)’ is extremely low. The SR of ‘GAE’ is much higher, as GAE can balance the variance and bias of policy gradient estimates. Nonetheless, GAE does not take the different action duration of SMDPs into consideration. Hence, AED with EGAE achieves the highest SR.

VII. REAL-WORLD EVALUATION

As illustrated in Figure 6, we also deploy the trained model of AED (0.4) and the trained model of 2D Baseline (0.4)³ to an actual differential-drive robot⁴ in the real world.

We place paper boxes as obstacles to set up spiral and zigzag environments. In addition, we also set up environments with scattered obstacles and pedestrians. Although we did not train our robot with dynamic obstacles, it is still able to avoid pedestrians successfully with a security policy. We use the value of total wall time (WT) and the average planning time (PT) to evaluate the trained models. Table IV summarizes the experimental results. The results show that AED works in more scenarios and takes less WT and PT to reach the target – AED can not only perform more difficult navigation tasks in unknown scenarios but also navigate faster with less computational overhead. Finally, AED can enable the robot to rapidly adapt to its environments by dynamically adjusting the execution duration. The demonstration video on both simulation and real-world experiments can be found at <https://youtu.be/toip5bFfJ1w>.

³We did not deploy 2D Baseline (0.8) to the actual robot because it greatly increases the risk of collision in the real world and [14] deployed 2D Baseline (0.4) to their robots.

⁴The robot executes actions discretely in every 0.1 second, which is the maximum frequency supported by the robot.

TABLE II

SUCCESS RATE OF DIFFERENT METHODS ON TESTING SCENARIOS.

Method	Param.	scenario				
		Sparse	Dense	Spiral	Zigzag	Average
DWA (Δt)	0.1	0.412	0.670	0	0	0.271
	0.2	0.616	0.618	0	0	0.309
	0.4	0.432	0.762	0	0	0.299
2D Base (Δt)	0.1	0.004	0.070	0	0	0.019
	0.2	0.452	0.648	0	0	0.275
	0.4	0.782	0.760	0	0	0.386
	0.8	0.964	0.754	0.792	0.836	0.837
	1.2	0.938	0.734	0.788	0.716	0.794
	1.6	0.680	0.524	0.018	0	0.306
3D Base ($\delta t \times n$)	0.1*20	0.430	0.434	0	0	0.216
	0.2*10	0.775	0.752	0	0	0.382
	0.4*5	0.860	0.854	0.104	0	0.455
AED (τ^{TP})	0.1	0.644	0.624	0.374	0.050	0.423
	0.2	0.924	0.846	0.994	0.642	0.852
	0.3	0.922	0.848	1.00	0.826	0.900
	0.4	0.946	0.910	1.00	0.904	0.940
	0.5	0.922	0.884	0.992	0.748	0.887
	0.6	0.922	0.850	0.964	0.812	0.887
	0.8	0.902	0.772	0.872	0.848	0.849

TABLE III

RESULTS OF AN ABLATION STUDY. WE SHOW SR VALUES OF DIFFERENT METHODS.

Method	scenario				
	Sparse	Dense	Spiral	Zigzag	Average
ReLu	0.936	0.840	0.990	0.532	0.825
TD(0)	0.760	0.646	0.228	0	0.409
GAE	0.944	0.906	1.00	0.804	0.913
AED	0.946	0.910	1.00	0.904	0.940

TABLE IV

AVERAGE WALL TIME (WT) AND PLANNING TIME (PT) OF METHODS IN REAL-WORLD SCENARIOS

Method	Metrics	Scenario		
		Scatter	Spiral	Zigzag
Baseline	WT	20.20	fail	fail
	PT	9.79	fail	fail
AED	WT	19.20	24.06	28.17
	PT	1.30	4.14	1.24

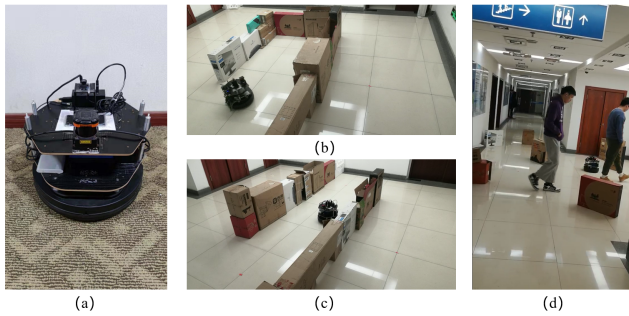


Fig. 6. We also conduct real-world experiments on a TurtleBot 2 with a Kobuki base using a Hokuyo UTM-30LX 2D LiDAR and a NVIDIA Jetson TX2 (shown in (a)). We consider three scenarios: Spiral (b), Zigzag (c), and scattered (d) (with scattered obstacles and pedestrians).

VIII. CONCLUSION

In this paper, we argue that the length of execution duration is crucial to the performance of DRL-based robot navigation – adopting adaptive execution duration is highly advantageous. Further, to better handle adaptive execution duration, we formulate the robot navigation task as a SMDP problem. In particular, we propose a DPPO-based navigation method, AED, which enables the robot to rapidly adapt to unknown environments by dynamically adjusting execution duration. Additionally, we introduce EGAE for better advantage function estimation in SMDP, as well as a transformation that converts 3D executable actions to 2D virtual actions for reduced training difficulty. We show that AED outperforms several baseline schemes under multiple scenarios both in simulation and on a differential drive mobile robot. We also conduct ablation experiments that indicate the effectiveness of our improvements.

Our limitations are mainly in the following two aspects. Firstly, we have not considered the acceleration limits of physical robots, which could lead to a gap between simulation and real-world experiments. Secondly, the lack of training with moving obstacles makes it rely on security policies to avoid moving objects. As a consequence, it may not work efficiently in crowds. Therefore, we will try to solve these two problems in our future work.

REFERENCES

- [1] S. M. LaValle, *Planning algorithms*. Cambridge university press, 2006.
- [2] L. Tai, G. Paolo, and M. Liu, “Virtual-to-real deep reinforcement learning: Continuous control of mobile robots for mapless navigation,” in *Proceedings of the 30th International Conference on Intelligent Robots and Systems (IROS-2017)*. IEEE, 2017, pp. 31–36.
- [3] M. Pfeiffer, S. Shukla, M. Turchetta, C. Cadena, A. Krause, R. Siegwart, and J. Nieto, “Reinforced imitation: Sample efficient deep reinforcement learning for mapless navigation by leveraging prior demonstrations,” *IEEE Robotics and Automation Letters*, vol. 3, no. 4, pp. 4423–4430, 2018.
- [4] E. Marchesini and A. Farinelli, “Discrete deep reinforcement learning for mapless navigation,” in *Proceedings of the 37th International Conference on Robotics and Automation (ICRA-2020)*. IEEE, 2020, pp. 10 688–10 694.
- [5] D. V. Lu, D. Hershberger, and W. D. Smart, “Layered costmaps for context-sensitive navigation,” in *Proceedings of the 27th International Conference on Intelligent Robots and Systems (IROS-2014)*. IEEE, 2014, pp. 709–715.

- [6] S. J. Bradtke and M. O. Duff, “Reinforcement learning methods for continuous-time markov decision problems,” in *Proceedings of the 9th Neural Information Processing Systems (NeurIPS-1995)*, 1995, pp. 393–400.
- [7] S. Mahadevan and N. Khaleeli, “Robust mobile robot navigation using partially-observable semi-markov decision processes,” *Internal report*, 1999.
- [8] O. Saha and P. Dasgupta, “Real-time robot path planning around complex obstacle patterns through learning and transferring options,” in *Proceedings of the 17th International Conference on Autonomous Robot Systems and Competitions (ICARSC-2017)*. IEEE, 2017, pp. 278–283.
- [9] O. Saha, P. Dasgupta, and B. Woosley, “Real-time robot path planning from simple to complex obstacle patterns via transfer learning of options,” *Autonomous Robots*, vol. 43, no. 8, pp. 2071–2093, 2019.
- [10] J.-L. Blanco, J. González, and J.-A. Fernández-Madrugal, “Extending obstacle avoidance methods through multiple parameter-space transformations,” *Autonomous Robots*, vol. 24, no. 1, pp. 29–48, 2008.
- [11] N. Heess, D. TB, S. Sriram, J. Lemmon, J. Merel, G. Wayne, Y. Tassa, T. Erez, Z. Wang, S. M. A. Eslami, M. A. Riedmiller, and D. Silver, “Emergence of locomotion behaviours in rich environments,” *arXiv preprint arXiv:1707.02286*, 2017.
- [12] J. Schulman, P. Moritz, S. Levine, M. Jordan, and P. Abbeel, “High-dimensional continuous control using generalized advantage estimation,” in *Proceedings of the 4th International Conference on Learning Representations (ICLR-2016)*, 2016.
- [13] D. Fox, W. Burgard, and S. Thrun, “The dynamic window approach to collision avoidance,” *IEEE Robotics & Automation Magazine*, vol. 4, no. 1, pp. 23–33, 1997.
- [14] G. Chen, S. Yao, J. Ma, L. Pan, Y. Chen, P. Xu, J. Ji, and X. Chen, “Distributed non-communicating multi-robot collision avoidance via map-based deep reinforcement learning,” *Sensors*, vol. 20, no. 17, p. 4836, 2020.
- [15] X. Xiao, B. Liu, G. Warnell, and P. Stone, “Motion control for mobile robot navigation using machine learning: a survey,” *The International Journal of Robotics Research*, 2020.
- [16] M. Everett, Y. F. Chen, and J. P. How, “Collision avoidance in pedestrian-rich environments with deep reinforcement learning,” *IEEE Access*, vol. 9, pp. 10 357–10 377, 2021.
- [17] T. Fan, P. Long, W. Liu, and J. Pan, “Distributed multi-robot collision avoidance via deep reinforcement learning for navigation in complex scenarios,” *The International Journal of Robotics Research*, p. 0278364920916531, 2020.
- [18] B. Okal and K. O. Arras, “Learning socially normative robot navigation behaviors with bayesian inverse reinforcement learning,” in *Proceedings of the 33th International Conference on Robotics and Automation (ICRA-2016)*. IEEE, 2016, pp. 2889–2895.
- [19] O. Saha and P. Dasgupta, “Improved reward estimation for efficient robot navigation using inverse reinforcement learning,” in *Proceedings of the 12th NASA/ESA Conference on Adaptive Hardware and Systems (AHS-2017)*. IEEE, 2017, pp. 245–252.
- [20] N. Metropolis and S. Ulam, “The monte carlo method,” *Journal of the American statistical association*, vol. 44, no. 247, pp. 335–341, 1949.
- [21] D.-A. Clevert, T. Unterthiner, and S. Hochreiter, “Fast and accurate deep network learning by exponential linear units (ELUs),” 2016.
- [22] G. Bradski and A. Kaehler, *Learning OpenCV: Computer vision with the OpenCV library*. O’Reilly Media, Inc., 2008.
- [23] M. Abadi, P. Barham, J. Chen, Z. Chen, A. Davis, J. Dean, M. Devin, S. Ghemawat, G. Irving, M. Isard *et al.*, “Tensorflow: A system for large-scale machine learning,” in *Proceedings of the 12th USENIX symposium on operating systems design and implementation (OSDI-2016)*, pp. 265–283.
- [24] D. P. Kingma and J. Ba, “Adam: A method for stochastic optimization,” in *Proceedings of the 3rd International Conference on Learning Representations, (ICLR-2015)*, Y. Bengio and Y. LeCun, Eds., 2015.
- [25] V. Nair and G. E. Hinton, “Rectified linear units improve restricted boltzmann machines,” in *Proceedings of the 27th International Conference on Machine Learning (ICML-2010)*.